Non-local parallel transport in the tokamak scrape-off layer

J.T. Omotani[1], N.R. Walkden[1,2], B.D. Dudson[1], G. Fishpool[2]

[1]*York Plasma Institute, Department of Physics, University of York, Heslington, York, YO10 5DD, UK*

[2]*EURATOM/CCFE Fusion Association, Culham Science Centre, Abingdon, OX14 3DB, UK*

The heat and particle fluxes to the divertor components from the plasma exhaust place strong constraints on the design of future tokamak fusion reactors, from ITER onwards. It is therefore important to understand and be able to model transport in the scrape-off layer (SOL). Near the divertor the SOL plasma would ideally be relatively cold (and hence collisional), but near the mid-plane it would be too hot for (local) fluid models derived in the collisional limit to be accurate, while the strong parallel gradients on open field lines demand an accurate description of the parallel dynamics. The perpendicular evolution is dominated by turbulence and moreover is intermittent due to the formation and motion of large-scale coherent structures (filaments); fluid simulations are required to cover sufficient spatial and temporal scales to describe the transport. Kinetic corrections to the parallel transport that can be incorporated into three-dimensional fluid simulations are therefore required to give a realistic model of the SOL plasma; these can be provided by using a non-local model.

1 Non-local parallel closures

Here we give only a brief outline of the derivation of the non-local model; for more details see [1, 2]. Solving the one-dimensional kinetic equation

$$v_\parallel \frac{\partial \langle \delta f_e \rangle}{\partial \ell} = \sum_{a=e,i} C\left(\langle f_e^{(0)} + \delta f_e \rangle, \langle f_a^{(0)} + \delta f_a \rangle \right) - v_\parallel \frac{\partial \langle f_e^{(0)} \rangle}{\partial \ell} \tag{1}$$

determines the non-Maxwellian part δf_e from the evolved moments (density, fluid velocity and temperature), giving a closure for the fluid equations. C is the full, linearized Fokker-Planck collision operator but time derivatives are neglected as the electron thermal motion is much faster than the evolution of the background fields. Taking moments and truncating to L angular harmonics and K speed polynomials (indices $A, B, \ldots$ represent pairs (l,k) with $0 < l < L$, $0 < k < K$ for brevity) gives a set of moment equations. These can then be decoupled by transforming to a basis of the eigenvectors $W^A_{(B)}$ (whose eigenvalues are $\zeta_{(B)}$) of the matrix $C^{-1}\Psi$

$$\sum_B \Psi^A{}_B \frac{\partial n^B}{\partial z} = \sum_B C^A{}_B n^B + g^A \quad \longrightarrow \quad \zeta_{(A)} \frac{\partial \hat{n}^A}{\partial z} = \hat{n}^A + \hat{g}^A \tag{2}$$

where z is the dimensionless length given by normalizing to the collision length, $\frac{\partial \ell}{\partial z} = \lambda_C$. Taking a large enough number of moments allows the validity of the closures to be extended to

arbitrarily low collisionality (the simulations in Section 2 use $L = K = 10$, i.e. 100 moments). The drive term g^A, which is the moment expansion of $-v_\parallel \frac{\partial \langle f_e^{(0)} \rangle}{\partial \ell}$, receives contributions from the temperature gradient, velocity gradient and velocity: $g^A = g^A_{\nabla T} + g^A_{\nabla V} + g^A_{\delta V}$ with

$$g^{(l,k)}_{\nabla T} = \frac{5}{4}\frac{n_e}{T_e}\frac{\partial T_e}{\partial z}\delta^l_1\delta^k_1 \tag{3}$$

$$g^{(l,k)}_{\nabla V} = -\frac{1}{2}\frac{n_e}{v_{Te}}\frac{\partial V_{e\parallel}}{\partial z}\delta^l_2\delta^k_0 \tag{4}$$

$$g^{(l,k)}_{\delta V} = -\frac{2}{\sqrt{\pi}}\frac{n_e\left(V_{e\parallel} - V_{i\parallel}\right)}{v_{Te}}\delta^l_1\frac{(k+\frac{1}{2})!}{k!} \tag{5}$$

The solutions of the decoupled equations can be written explicitly as spatial integrals

$$\hat{n}^A(z) = \begin{cases} -\hat{g}^A & \zeta_{(A)} = 0 \\ \hat{n}^A(z_0)\exp\left(\frac{z-z_0}{\zeta_{(A)}}\right) + \int_{z_0}^{z} dz' \exp\left(\frac{z-z'}{\zeta_{(A)}}\right)\frac{\hat{g}^A(z')}{\zeta_{(A)}} & \zeta_{(A)} \neq 0 \end{cases} \tag{6}$$

The moments needed for parallel closures of the 3-moment fluid equations (for n_e, $V_{e\parallel}$ and T_e) are the heat-flux, viscosity and friction, which are given by

$$q_{e\parallel} = -\frac{5}{4}v_{Te}T_e n^{(1,1)} = -\frac{5}{4}v_{Te}T_e\sum_B W^{(1,1)}{}_B\hat{n}^B \tag{7}$$

$$\pi_{e\parallel,\parallel} = T_e n^{(2,0)} = T_e\sum_B W^{(2,0)}{}_B\hat{n}^B \tag{8}$$

$$R_{e\parallel} = -\frac{m_e n_e v_{Te}}{\lambda_{Cei}}\left(V_{e\parallel} - V_{i\parallel}\right) + \frac{m_e v_{Te}^2}{\lambda_{Cee}}\sum_{k>0} C^{(1,0)}{}_{(1,k)}\sum_B W^{(1,k)}{}_B\hat{n}^B \tag{9}$$

In summary, this method gives the closures for the fluid equations as sums of integrals, with LK integrals needed to evaluate them. In [1] only $g^A_{\nabla T}$ and $q_{e\parallel}$ were used; the full set of terms has now been implemented in BOUT++.

This non-local model allows a more accurate description of parallel heat conduction to be included in fluid simulations and so will be important for more realistic three-dimensional simulations of SOL transport, especially during ELMs. However, this aspect has already been discussed in detail in [1], so here we proceed directly to new work modelling current evolution.

2 Resistive drift wave instability

Drift waves are driven by pressure gradients. Without dissipation the fluctuations in density and potential are in phase and the wave does not grow; the phase shift (introduced for example by resistivity) drives the instability, and so simulation of a drift wave tests the accuracy of phase in BOUT++[3]. Since the dynamics of the system is determined solely by the resistivity and also requires only a minimal set of equations and a two-dimensional simulation domain, this system is a convenient place both to test the new additions to the non-local code and to begin examining the impact of kinetic corrections in parallel dynamics on the perpendicular transport.

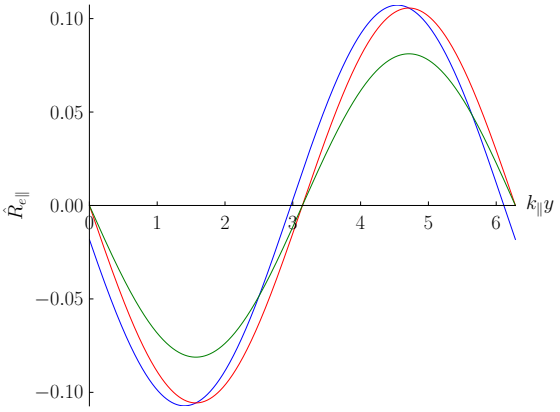

Figure 1: Normalized friction for sinusoidal velocity profile and $k_\| = k_C$, non-local model (blue), non-local model excluding $g^A_{\nabla V}$ (red), collisional (green)

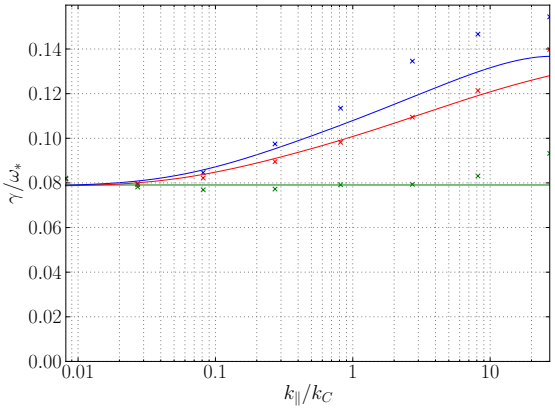

Figure 2: Drift wave growth rate, non-local model (blue), non-local model excluding $g^A_{\nabla V}$ (red), collisional (green). Crosses show simulation results, lines are the analytic predictions

The equations we use to describe a linear resistive drift wave instability are

$$\frac{\partial n_i}{\partial t} = -\mathbf{V}_E \cdot \nabla n_{i0} \tag{10}$$

$$\frac{\partial \varpi}{\partial t} = \frac{eB^2}{m_i c^2} \nabla_\| j_\| \tag{11}$$

$$\frac{\partial j_\|}{\partial t} = \frac{e n_{i0}}{m_e} \nabla_\| \left(e\phi - \frac{T_{e0}}{n_{i0}} n_i \right) + \frac{e}{m_e} R_{e\|} \tag{12}$$

with $\nabla n_{i0} = \frac{n_{i0}}{L_n}\hat{\mathbf{r}}$ driving the drift wave; $\varpi \equiv n_{i0} e \nabla^2_\perp \phi$ is the vorticity. The simulation domain is a doubly periodic box (normal to $\hat{\mathbf{r}}$) with lengths $L_\| \equiv \frac{2\pi}{k_\|}$ and $L_\perp \equiv \frac{2\pi}{k_\perp}$. In the collisional limit $R_{e\|} = R_{e\|,Brag} \equiv 0.51 \frac{m_e \nu_{ei}}{e} j_\|$ while for the non-local model $R_{e\|}$ is given by (9). $j_\|$ is evolved according to (12) rather than being determined algebraically (by Ohm's law) because (9) cannot be inverted for $j_\|$ as $R_{e\|,Brag}$ can be.

Neglecting electron inertia the dispersion relation is

$$(\omega - \omega_*)\, i\sigma_\| + \omega^2 = 0; \quad \omega_* \equiv \frac{k_\perp T_{e0}}{m_e \Omega_{ce} L_N} \tag{13}$$

and in the collisional limit $\sigma_\| \equiv \left(\frac{k_\|}{k_\perp}\right)^2 \frac{\Omega_{ci}\Omega_{ce}}{0.51 \nu_{ei}}$. For the non-local model, assuming a purely sinusoidal perturbation, $V_e = V_0 \sin(k_\| l_\|)$, allows the integrals in (6) to be evaluated analytically: the $g^A_{\delta V}$ drive (4) gives a contribution to the friction $\propto \frac{m_e \nu_{ei} V_0}{e} \sin(k_\| l_\|)$ with a coefficient depending on $\frac{k_\|}{k_C}$ which tends to 0.51 as $\frac{k_\|}{k_C}$ tends to 0; the $g^A_{\nabla V}$ drive (5) gives a contribution $\propto \frac{m_e \nu_{ei} V_0}{e} \cos(k_\| l_\|)$ with a coefficient depending on $\frac{k_\|}{k_C}$ which vanishes as $\frac{k_\|}{k_C}$ tends to 0. We scale $k_\|$ to vary the collisionality, keeping $k_\perp \propto k_\|^{2/3}$ so that $\frac{\sigma_{\|,Brag}}{\omega_*}$ is constant and the collisional model predicts the same growth rate, in units of ω_*, for every $k_\|$. As $k_\|$ increases to become comparable to $k_C = \frac{2\pi}{\lambda_C}$, the effect of the $g^A_{\delta V}$ contribution to (9) is to increase the magnitude of $\sigma_\|$ while the $g^A_{\nabla V}$ contribution introduces a small phase shift (making $\sigma_\|$ complex), as illustrated

in Figure 1. These effects both (for the parameters used here) enhance the growth rate of the instability, as we see in Figure 2, which shows that simulations of the collisional model and the non-local model excluding $g^A_{\nabla V}$ both agree well with the analytical predictions while the simulations of the non-local model including $g^A_{\nabla V}$ show a further increase in the growth rate. We attribute this to the phase shift from $g^A_{\nabla V}$ causing the profiles to evolve away from the pure single mode (with $\frac{\pi}{2}$ phase shift in the current) assumed by the analytic prediction.

In three-dimensional simulations of filament evolution in the SOL of the MAST reactor[4], qualitatively different regimes are observed, with the transition between them characterized by decreasing collisionality that switches off the resistive (friction) term in Ohm's law. The sorts of changes to the friction described above would be expected to become significant at intermediate collisionalities, and so might have an effect on the position of the transition, shifting it to lower collisionality as the resistivity would be enhanced. It also seems likely that a non-local model would have some effects on the details of the filament dynamics, especially as there are several distinct parallel length scales present in this case.

3 Conclusions and ongoing work

We have now implemented a complete set of non-local parallel closures for (three-moment) electron fluid equations in BOUT++ so that kinetic effects on both heat conduction and resistivity can be included in simulations. Both types of kinetic correction may be expected to be important for fusion relevant parameter regimes, especially in the SOL where there is strong variation along magnetic field lines. The code is efficiently parallelized to enable large scale three-dimensional simulations to be performed with self consistent coupling of kinetically-corrected parallel transport to turbulent perpendicular transport.

We are currently working on including these non-local closures in three-dimensional simulations of the MAST SOL, building on those described in [4], to extend their validity to lower collisionalities and allow realistic simulation of ELM filaments. Other topics of interest include: detailed validation of the non-local model against fully kinetic (PIC) simulations; improved fluid models for sheath boundary conditions, including some kinetic corrections; and implementation on closed, non-periodic flux surfaces to allow the non-local code to be used in edge simulations to study, for instance, ELM dynamics and stochastic field lines.

References

[1] J.T. Omotani and B.D. Dudson. *Plasma Physics and Controlled Fusion*, 55(5):055009, 2013.

[2] J.Y. Ji, E.D. Held, and C.R. Sovinec. *Physics of Plasmas*, 16(2):022312, 2009.

[3] B.D. Dudson et al. *Computer Physics Communications*, 180:1467–1480, 2009.

[4] N.W. Walkden, B.D. Dudson, and G. Fishpool. *EPS Conference on Plasma Physics 2013*, O4.106.